Structural Characterization of the Cell Surface Lipooligosaccharides from a Nontypable Strain of *Haemophilus influenzae*†

Nancy J. Phillips,‡ Michael A. Apicella,§ J. McLeod Griffiss,‖ and Bradford W. Gibson*,‡

Department of Pharmaceutical Chemistry, University of California, San Francisco, California 94143, Department of Medicine, State University of New York, Buffalo, New York 14215, and Centre for Immunochemistry, Department of Laboratory Medicine and Veterans Affairs Medical Center, University of California, San Francisco, California 94143

Received December 2, 1991; Revised Manuscript Received February 19, 1992

ABSTRACT: Oligosaccharides released from the lipooligosaccharides (LOS) of *Haemophilus influenzae* nontypable strain 2019 by mild acid hydrolysis were fractionated by size exclusion chromatography and analyzed by liquid secondary ion mass spectrometry. The major component of the heterogeneous mixture was found to be a hexasaccharide of M_r 1366, which lost two phosphoethanolamine groups upon treatment with 48% aqueous HF. The dephosphorylated hexasaccharide was purified and shown by tandem mass spectrometry, composition analysis, methylation analysis, and two-dimensional nuclear magnetic resonance studies to be Galβ1→4Glcβ1→(Hepα1→2Hepα1→3)4Hepα1→5anhydro-KDO, where Hep is L-*glycero*-D-*manno*-heptose and KDO is 3-deoxy-D-*manno*-octulosonic acid. An analogous structure containing authentic KDO was generated from LOS that had been HF-treated prior to acetic acid hydrolysis, suggesting that the reducing terminal anhydro-KDO moiety is produced as an artifact of the hydrolysis procedure by β-elimination of a phosphate substituent from C-4 of KDO. Mass spectral analyses of *O*-deacylated LOS and free lipid A confirmed that, in addition to the two phosphoethanolamines on the oligosaccharide and two phosphates on the lipid A, another phosphate group exists on the KDO. This KDO does not appear to be further substituted with additional KDO residues in intact *H. influenzae* 2019 LOS. The terminal disaccharide epitope, Galβ1→4Glcβ1→, of the hexasaccharide is also present on lactosylceramide, a precursor to human blood group antigens. It is postulated that the presence of this structure on *H. influenzae* LOS may represent a form of host mimicry by the pathogen.

Haemophilus influenzae is a Gram-negative pathogen which colonizes the human upper respiratory tract. The bacterium is found in both encapsulated and unencapsulated (nontypable) forms, which differ significantly in their ability to cause disease and evade the host's immune system (Mäkelä, 1988; Moxon, 1990). In developed countries, *H. influenzae* type b (Hib),[1] a capsular serotype, is the leading cause of bacterial meningitis in young children. The capsular polysaccharide of this organism plays a critical role in mediating the virulence of Hib (Moxon & Vaughn, 1981). Nontypable strains of *H. influenzae* (NTHI), which are commonly present in the nasopharynx of 50–80% of healthy carriers (Turk, 1982), have only recently been recognized to be important human pathogens. Both invasive diseases and localized infections of the respiratory tract are caused by NTHI (Murphy & Apicella, 1987). Since NTHI lacks a capsular polysaccharide, its pathogenicity is mediated more directly by surface components of the bacterial outer membrane, including proteins and lipooligosaccharides (LOS) (Campagnari et al., 1987; Patrick et al., 1987).

Like the LOS of *Neisseria gonorrhoeae*, *Neisseria meningitidis*, and *Bordetella pertussis*, the LOS of *H. influenzae* do not contain the repeating oligosaccharide units (O-antigens) characteristic of the lipopolysaccharides (LPS) made by enteric bacteria. Rather, the LOS of these mucosal pathogens contain short, multiantennary glycans similar to those found in rough mutants of enteric bacteria which lack O-antigens. A single strain of *H. influenzae* generally produces a heterogeneous mixture of LOS with oligosaccharides (OS) of different sizes (Campagnari et al., 1987; Patrick et al., 1987, 1989). An understanding of the precise structural features of the OS moieties of LOS is essential to identifying surface-exposed epitopes available for host/pathogen interactions.

A structural model for neisserial LOS has been constructed (Phillips et al., 1990) based on published oligosaccharide (Jennings et al., 1980, 1983; Gibson et al., 1989; Di Fabio et al., 1990; Yamasaki et al., 1991) and lipid A structures (Takayama et al., 1986). To date, much less is known about the LOS from *H. influenzae*. Various groups have studied the chemical composition of Hib LOS (Flesher & Insel, 1978;

† Financial support was provided by grants from the National Institute of Allergy and Infectious Diseases (AI21620 and AI24616). We also acknowledge support from the National Institutes of Health (RR01640), the National Science Foundation Instrumentation Program, and the Research Service of the Department of Veterans Affairs. This is Report No. 55 from the Centre for Immunochemistry of the University of California, San Francisco.

* To whom correspondence should be addressed at the School of Pharmacy 926-S, 513 Parnassus Ave., University of California, San Francisco, CA 94143-0446.

‡ Department of Pharmaceutical Chemistry, UCSF.

§ SUNY at Buffalo.

‖ Department of Laboratory Medicine and Veterans Affairs Medical Center, UCSF.

[1] Abbreviations: 1D, one dimensional; 2D, two dimensional; COSY, 2D *J*-correlated spectroscopy; DQF-COSY, double-quantum filtered COSY; Gal, galactose; GalNAc, *N*-acetylgalactosamine; Glc, glucose; GlcNAc, *N*-acetylglucosamine; HBEE, ethyl 4-hydrazinobenzoate; Hep, L-*glycero*-D-*manno*-heptose; Hex, hexose; HexNAc, *N*-acetylhexosamine; Hib, *Haemophilus influenzae* type b; HOHAHA, 2D homonuclear Hartmann–Hahn spectroscopy; KDO, 3-deoxy-D-*manno*-octulosonic acid; LOS, lipooligosaccharide; LPS, lipopolysaccharide; LSIMS, liquid secondary ion mass spectrometry; $(M-H)^-$, deprotonated molecular ion; MS/MS, tandem mass spectrometry; NMR, nuclear magnetic resonance; NOE, nuclear Overhauser effect; NOESY, 2D NOE spectroscopy; NTHI, nontypable *Haemophilus influenzae*; OS, oligosaccharide; PEA, phosphoethanolamine; PPEA, pyrophosphoethanolamine.

0006-2960/92/0431-4515$03.00/0

Parr & Bryan, 1984; Inzana et al., 1985; Zamze & Moxon, 1987; van Alphen et al., 1990) and the LOS from other serotype strains (Zamze & Moxon, 1987). Glucose, galactose, and L-*glycero*-D-*manno*-heptose have been consistently observed, along with glucosamine and/or galactosamine in some strains. Phosphate and phosphoethanolamine are also common constituents. 3-Deoxy-D-*manno*-octulosonic acid (KDO), a nearly universal component of bacterial LPS, could not be readily detected in *H. influenzae* LOS using the traditional thiobarbituric acid assay (Flesher & Insel, 1978; Zamze & Moxon, 1987). This suggested that KDO was either absent from *H. influenzae* LOS or modified. Using an alternate semicarbazide assay and gas chromatography–mass spectrometry (GC/MS), the presence of KDO in Hib strain Eagan was confirmed by Inzana et al. (1985). Subsequently, phosphorylated KDO was identified in the LOS from a deep-rough genetically engineered strain of *H. influenzae* (Rb^+I69) (Zamze et al., 1987). The LOS from this strain was later shown to contain a truncated OS moiety containing only a single KDO, which was found to be phosphorylated on either C-4 or C-5 (Helander et al., 1988). We now report the structural characterization of the LOS from a wild-type NTHI strain (strain 2019) which contains a much larger oligosaccharide moiety, yet also possesses a "KDO-related" epitope associated with the LOS of two recombinant *H. influenzae* strains (Spinola et al., 1990; Campagnari et al., 1990).

Experimental Procedures

Materials

LPS from *Salmonella typhimurium* TV119 Ra mutant, galactose, glucose, galactosamine, glucosamine, 3-deoxy-D-*manno*-octulosonic acid (KDO) and anhydrous hydrazine were all obtained from Sigma (St. Louis, MO). Aqueous HF (48%) was purchased from Mallinckrodt (Muskegon, MI), acetic anhydride from Supelco (Bellefonte, PA), and iodomethane from Fluka (Buchs, Switzerland). Sodium hydroxide pellets (99.9%) and sodium borodeuteride (98% D) were purchased from Aldrich (Milwaukee, WI). The standard mixture of partially methylated alditol acetates used for GC/MS analysis was obtained from Biocarb (Lund, Sweden). 18-MΩ water required for the Dionex chromatography was generated from deionized water using a Millipore milli-Q water purification system. Acetonitrile, water, methanol, and methylene chloride were obtained from Burdick and Jackson (Muskegon, MI). All other reagents and solvents used were of reagent grade.

Methods

Isolation and Purification of LOS. The LOS of *H. influenzae* nontypable strain 2019 (NTHI 2019) was prepared using the extraction procedure of Darveau and Hancock (1983). Briefly, this method uses sequential enzyme digestions to remove RNA, DNA, peptidoglycan, and bacterial proteins. The LOS is then extracted from the denatured proteins by SDS extraction, followed by extensive dialysis and precipitation with ethanol (Darveau & Hancock, 1983). The isolated LOS was analyzed by sodium dodecyl sulfate–polyacrylamide gel electrophoresis (SDS–PAGE) and found to consist of one major component and several minor species (Campagnari et al., 1990), with the major component appearing roughly comparable in size to the *Salmonella minnesota* Rb mutant.

Isolation of OS from LOS. The LOS from NTHI 2019 (32 mg) and commercially available *S. typhimurium* TV119 Ra mutant (20 mg) were hydrolyzed in 1% acetic acid (2 mg of LOS/mL) for 2 h at 100 °C with stirring. The hydrolysates were centrifuged at 5000*g* for 20 min at 4 °C, and the supernatants were removed. Pellets were washed (one or two times) with 1–3 mL of H_2O and centrifuged again (5000*g*, 20 min, 4 °C). The supernatants and washings were pooled and lyophilized. The lyophilized OS fractions were redissolved in 0.5–1 mL of H_2O and centrifuge-filtered using Microfilterfuge tubes with 0.45-μm Nylon-66 membrane filters (Rainin). *H. influenzae* 2019 OS fractions often contained traces of SDS which could be removed by passing the OS (dissolved in 1 mL of H_2O) through a C_{18} Sep-Pak (Waters Associates) and eluting with 3–4 mL of H_2O.

Gel Filtration Chromatography. The NTHI 2019 OS fraction (11.5 mg) was dissolved in 0.3 mL of 0.05 M pyridinium acetate buffer (pH 5.2), centrifuge-filtered, and applied to two Bio-Gel P-4 columns connected in series (1.6 × 79 cm and 1.6 × 76.5 cm, <400 mesh; Bio-Rad). The columns were equipped with water jackets maintained at 30 °C. Upward elution at a flow rate of ≈10 mL/h was achieved with a P-1 peristaltic pump (Pharmacia), and fractions were collected at 10-min intervals and evaporated to dryness in a Speed-Vac concentrator. A refractive index detector (Knauer) was used to monitor column effluent, and chromatograms were recorded and stored with a Shimadzu C-R3A Chromatopac integrator. Selected OS fractions were pooled, dephosphorylated, and fractionated again on a Bio-Gel P-4 column (1.6 × 84 cm) as described above.

OS samples weighing less than 1–2 mg were alternatively purified by a gel filtration HPLC system employing a Waters 6000A HPLC pump and two 600 × 7.5 mm Bio-Sil TSK-125 columns (Bio-Rad) connected in series. Samples were eluted in 1% acetic acid or 0.05 M pyridinium acetate (pH 5.2) at a flow rate of 1 mL/min. Fractions were collected in 0.5–1-mL volumes, and detection was as described above.

High-Performance Anion Exchange Chromatography with Pulsed Amperometric Detection. Anion exchange chromatography was performed using a Dionex BioLC (Dionex, Sunnyvale, CA). The system was equipped with a gradient pump, pulsed amperometric detector, and CarboPak PA1 column (4 × 250 mm). The following pulse potentials and durations were used for detection: $E_1 = 0.05$ V ($t_1 = 480$ ms); $E_2 = 0.60$ V ($t_2 = 120$ ms); $E_3 = -0.60$ V ($t_3 = 60$ ms). The response time of the PAD was set to 3 s, and an output range of 300 or 1000 nA was typically used. As previously described (Phillips et al., 1990), the four standard eluents used were H_2O, 1 M NaOH, 200 mM NaOH, and 1 M NaOAc. A Dionex anion micromembrane suppressor was used when collection of desalted samples was undertaken. The dephosphorylated NTHI 2019 hexasaccharide (≈2 μg) was eluted using the following gradient: (1) 16 mM NaOH for 15 min, (2) linear to 100 mM NaOH in 10 min, (3) linear to 500 mM NaOAc in 30 min while holding 100 mM NaOH constant. The same separation was obtained when gradient steps 1 and 2 were decreased to 5 min each.

For composition analysis, ≈15 nmol of the dephosphorylated NTHI 2019 hexasaccharide was dissolved in 200 μL of H_2O, treated with 200 μL of 4 M trifluoroacetic acid, and heated for 4.5 h at 100 °C. The hydrolysate was evaporated to dryness in a Speed-Vac concentrator, redissolved in 20 μL H_2O, and dried again. For anion exchange chromatography, the sample was dissolved in 100 μL of H_2O, and 20 μL was injected. To elute all the monosaccharide components, the following gradient was used: (1) 16 mM NaOH for 20 min, (2) linear to 40 mM NaOH in 10 min, (3) linear to 100 mM NaOH and 100 mM NaOAc in 5 min, and (4) linear to 160 mM NaOAc in 15 min while holding 100 mM NaOH constant. Response factors for the various monosaccharides were

determined with a standard monosaccharide mixture containing $GalNH_2$, $GlcNH_2$, Gal, Glc, and KDO. Approximately 10 nmol of the dephosphorylated OS from *S. typhimurium* Ra mutant was hydrolyzed under the same conditions to provide authentic L-*glycero*-D-*manno*-heptose.

Derivatization of Oligosaccharides with Ethyl 4-Hydrazinobenzoate (HBEE) and HPLC Purification. Oligosaccharides (10–100 nmol) were dissolved in 10 μL of H_2O and placed in 1-mL glass Reacti-Vials. Approximately 3 molar equiv of HBEE reagent in 40 μL of methanol was added to each sample, followed by ≈0.5 μL of glacial acetic acid. The reaction mixtures were placed in a heating block at 80 °C for 30 min, cooled, and then dried under a stream of N_2. The derivatized OS samples were redissolved in H_2O and separated using a Rainin HPLC system with a reverse-phase C_{18} column (Vydac, 25 cm × 4.6 mm i.d.). The HBEE-OS were eluted with a linear gradient of H_2O to 50% CH_3CN in 50 min at a flow rate of 1 mL/min and detected at 320 nm with a Kratos 783 variable wavelength detector. Both HPLC solvents contained 0.05% trifluoroacetic acid (John & Gibson, 1990).

O-Deacylation of LOS. The NTHI 2019 LOS sample was *O*-deacylated following the procedure of Helander et al. (1988). Approximately 11 mg of LOS was placed in a 25-mL glass centrifuge tube and treated with 1.1 mL of anhydrous hydrazine. The sample was shaken at 37 °C in a water bath for 20 min with occasional sonication and then cooled to −20 °C and diluted with 5.5 mL of chilled acetone (−20 °C), added dropwise. The precipitated *O*-deacylated LOS was centrifuged at 12000*g* for 20 min, and the supernatant was removed. The pellet was washed with cold acetone and centrifuged a second time. Finally, the precipitated *O*-deacylated LOS was dissolved in 500 μL of H_2O, frozen, and lyophilized.

HF-Treatment of Oligosaccharides, O-Deacylated LOS, and LOS. LOS, *O*-deacylated LOS, or OS (0.1–1 mg) were placed in 1.5-mL polypropylene tubes. In an ice bath, samples were treated with cold 48% aqueous HF to make 5–10 μg/μL solutions. OS and *O*-deacylated LOS were then kept for 16–24 h at 4 °C; intact LOS were HF-treated for up to 48 h at 4 °C. Aqueous HF was evaporated under a stream of N_2 in a polypropylene desiccator containing NaOH pellets. The desiccator was connected to a water aspirator with an in-line NaOH trap.

Methylation Analysis. Linkage analysis was performed on purified OS using the microscale method of Levery and Hakomori (1987) modified for use with powdered NaOH (Larson et al., 1987). Given the resistance of Hep–Hep bonds to acid hydrolysis, the longer hydrolysis times (21 h) and slightly greater acidic conditions of the older Hakomori procedure (Stellner et al., 1973) were used. As described in detail elsewhere (Phillips et al., 1990), the OS were dissolved in DMSO and treated with powdered NaOH and CH_3I. After being stirred at room temperature for 45 min, the solutions were extracted with CH_2Cl_2/H_2O. The permethylated samples were hydrolyzed in 0.5 N sulfuric acid in 95% acetic acid for 16 h at 80 °C, diluted with an equal volume of H_2O, and heated for 5 h at 80 °C. The hydrolysates were partially neutralized using a NaOH solution (2.6 molar equiv relative to H_2SO_4), dried, and then reduced with $NaBD_4$ in 0.01 N NaOH at 4 °C overnight. The dried samples were then converted to their partially methylated alditol acetates by treatment with 300 μL of acetic anhydride at 100 °C for 2 h and analyzed by GC/MS on a VG70SE mass spectrometer. To determine the linkage position of the reducing terminal KDO moiety, two additional reduction steps were added to the methylation analysis procedure (York et al., 1985). As described elsewhere (John et al., 1991), the ketone of the KDO moiety was first reduced to a secondary alcohol with $NaBD_4$ prior to methylation. After methylation and before the hydrolysis step, the methyl ester of the permethylated KDO moiety was converted to a primary alcohol by reduction with $NaBD_4$.

Preparation of Alditol Acetates. OS from NTHI 2019 (36 μg) and *S. typhimurium* TV119 Ra mutant (50 μg) were hydrolyzed under the conditions used for composition analysis by anion exchange chromatography (described above). The monosaccharides were then reduced by treatment with 150 μL of 10 mg/mL $NaBD_4$ in 1 M NH_4OH for 2.3 h at room temperature. The reactions were quenched and worked up as in the methylation analysis procedure. Samples were then dried in vacuo over P_2O_5 for 2 h and peracetylated using the method described above. GC/MS analysis was performed using the conditions for partially methylated alditol acetates.

Nuclear Magnetic Resonance Spectroscopy. All 1D and 2D ^1H NMR spectra were recorded on a GE GN-500 spectrometer at 25 °C. The dephosphorylated NTHI 2019 hexasaccharide (1.5 mg) was lyophilized 3–4 times from 99.96% D_2O (Aldrich) and then dissolved in 0.3 mL of 99.996% D_2O (Merck Sharp & Dohme). A trace of acetone was added to the sample as an internal reference (δ 2.225). The phase-sensitive double-quantum filtered COSY (DQF-COSY) spectrum (Rance et al., 1983) was acquired with time-proportional phase incrementation of the first pulse (Redfield & Kuntz, 1975; Marion & Wüthrich, 1983). The data matrix consisted of 800 × 1024 data points, acquired with 16 scans per t_1 value and a spectral width of ±1506 Hz. The matrix was apodized with a 45°-shifted sine-bell window function in both dimensions and zero-filled to produce a 2K × 4K real data matrix. The 2D homonuclear Hartmann–Hahn (HOHAHA) spectrum was obtained using the MLEV-17 sequence (Bax & Davis, 1985) and quadrature detection method of States et al. (1982). A spectral width of ±1000 Hz was used, with a 90-ms relay mixing time. A data matrix of 456 × 2048 data points was acquired with 12 scans per t_1 increment. The matrix was zero-filled in the t_1 dimension and apodized with Gaussian window functions in both dimensions to give 1K × 2K real points. The phase-sensitive 2D nuclear Overhauser effect (NOESY) spectrum was acquired following the method of States et al. (1982), using a 400-ms mixing time and 2.8-s interscan delay. The spectral width was ±2000 Hz, and the data matrix contained 400 × 1024 data points, with 16 scans per t_1 value. Zero-filling and Gaussian apodization functions were used in both dimensions to give a final 2K × 2K matrix. All data processing was done on a VAX computer with a Unix operating system using programs developed and modified at the UCSF NMR facility as previously described by Basus et al. (1988), including some recent improvements (M. Day, unpublished data).

Liquid Secondary Ion Mass Spectrometry (LSIMS). LSIMS was performed using a Kratos MS50S mass spectrometer with a cesium ion source (Falick et al., 1986). To prepare samples for LSIMS analysis, ca. 1 μL of glycerol/thioglycerol (1:1) was applied to the stainless steel probe tip and aliquots of the sample solution (dissolved in H_2O) were added with intermittent drying. (To suppress undesired adduct ions, ≈0.5 μL of 0.1 N HCl was sometimes added to the matrix.) A Cs^+ ion primary beam energy of 10 keV was used, and the secondary sample ions were accelerated to 8 keV. Scans were taken in the negative-ion mode at 300 s/decade and recorded with a Gould ES-1000 electrostatic recorder. The spectra were mass calibrated manually with Ultramark

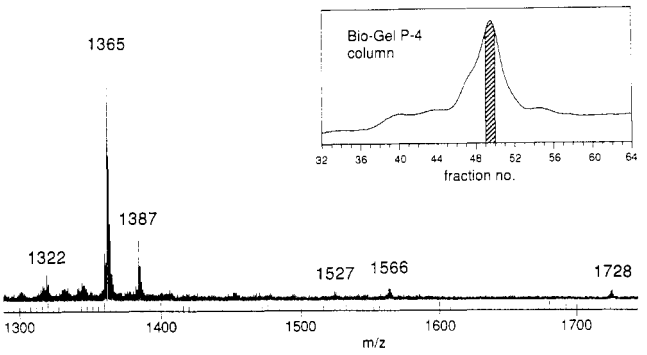

FIGURE 1: Partial negative-ion LSIMS spectrum of Bio-Gel P-4 column fraction number 49. (Inset) Oligosaccharide region of the Bio-Gel P-4 column elution profile. The elution volume of the major peak was 150 mL, and V_o and V_t for the column were ≈80 and 280 mL, respectively.

1621 to an accuracy of better than ±0.2 Da.

Tandem Mass Spectrometry (MS/MS). A four-sector mass spectrometer (Kratos Concept II HH, Kratos Analytical, Manchester, England) equipped with a 4% diode array detector on MS-II was used for all analyses as previously described (Walls et al., 1990). All samples were prepared as described above for the two-sector experiments. Spectra were taken in the negative-ion mode using a Cs^+ beam energy of 18 keV to produce abundant deprotonated molecular ions in MS-I. The isotopically pure ^{12}C component of the parent deprotonated molecular ion was then collisionally activated in the collision cell between MS-I and MS-II. The helium collision gas was used at a pressure sufficient to attenuate the parent ion beam to one-third of its initial value. The collision cell was floated at a potential of 2 kV, resulting in a collision energy of 6 keV. The fragment ions (or "daughter ions") resulting from decomposition of the collisionally activated parent ions were then mass analyzed and detected in MS-II. The magnet and electric sector of MS-II were stepped to produce a series of contiguous 4% mass frames. The mass scales on MS-I and MS-II were both calibrated with CsI using a Kratos Mach 3 data system as previously described (Walls et al., 1990).

Electrospray Mass Spectrometry. Samples were analyzed on a Bio-Q mass spectrometer (VG Instruments, Manchester, England) with an electrospray ion source. *O*-Deacylated LOS were first dissolved in H_2O and then diluted 1:1 with electrospray solvent (50:50 CH_3CN/H_2O with 1% HOAc). Five microliters was injected with a Rheodyne 8125 injector located downstream from a syringe pump set at 2.0 μL/min. The electrospray tip voltage was typically 4.0 kV. The mass spectrometer was scanned from m/z 400 to 2000 with a scan time of 10 s. Data were collected in multichannel analysis mode, and data processing was handled by the VG data system.

RESULTS

Oligosaccharides Released from the LOS of NTHI Strain 2019. Mild acid hydrolysis of the LOS generated a water-soluble OS fraction that produced a major peak with small shoulders when separated by Bio-Gel P-4 chromatography (Figure 1, inset). Fractions were dried and analyzed by liquid secondary ion mass spectrometry (LSIMS) in the negative-ion mode. Figure 1 shows the LSIMS spectrum of fraction 49, which represents the center of the OS peak. The major molecular ions observed in all of the oligosaccharide-containing column fractions are listed in Table I. As indicated, the principal component of the major peak (fractions 46–51) was an OS of M_r 1366.[2] Earlier eluting fractions contained higher molecular weight oligosaccharides representing minor components of the mixture.

Table I: Molecular Ions Detected in the Bio-Gel P-4 Column Fractions of the *H. influenzae* 2019 Oligosaccharide Mixture[a,b]

fraction no.	deprotonated molecular ions; $(M-H)^-$
37	2077,[c] 1407, 1245
38	2077,[c] 1730, 1530,[d] 1407, 1245
39	**2093**, 1915,[c] 1730, 1530,[d] 1407, 1245
40	**2093**, 1915,[c] 1591,[c] 1530,[d] 1322, 1245
41	1591,[c] 1530,[d] 1322
42	1851, 1591,[c] 1322
43	**1851**, **1591**,[c] 1365, 1322
44	**1851**, 1689, **1591**,[c] 1365
45	1851, 1689, 1407, 1365
46	1689, 1407, **1365**
47	1728, 1689, 1407, **1365**
48	1728, 1566, 1527, **1365**, 1322
49	1728, 1566, **1365**, 1322
50	1728, 1566, **1365**, 1322, 1203
51	1774,[d] 1566, **1365**, 1203
52	1774,[d] **1566**, 1404, 1365, 1242, **1203**
53	1612,[d] 1566, 1404, 1242, 1203
54	1612,[d] 1566, **1404**, 1242
55	1612,[d] **1404**, 1242
56	1404, 1242

[a] Masses are listed as the nominal mass values of the ^{12}C-containing isotope. Major components are listed in boldface type. [b] Most major species also gave sodiated molecular ions, $(M+Na-2H)^-$. Additionally, several species were detected as +226 Da[c] and +208 Da[d] adduct ions, whose ionization could be suppressed by acidification of the LSIMS matrix and whose mass increments are consistent with free fatty acids known to be present in the LOS preparation.

Table II: Molecular Weights and Proposed Compositions of the Major Oligosaccharides Present in the *H. influenzae* 2019 Sample[a]

$(M-H)^-$	M_r	proposed compositions
1203	1204	KDO*, Hep_3, Hex, PEA_2
1242	1243	KDO*, Hep_3, Hex_2, PEA
1245	1246	KDO*, Hep_3, Hex, PEA_2, Ac
1322	1323	KDO*, Hep_3, Hex_2, (P + PEA, or HexNAc)[b]
1365	1366	KDO*, Hep_3, Hex_2, PEA_2
1404	1405	KDO*, Hep_3, Hex_3, PEA
1407	1408	KDO*, Hep_3, Hex_2, PEA_2, Ac
1527	1528	KDO*, Hep_3, Hex_3, PEA_2
1566	1567	KDO*, Hep_3, Hex_4, PEA
1689	1690	KDO*, Hep_3, Hex_4, PEA_2
1728	1729	KDO*, Hep_3, Hex_5, PEA
1730	1731	KDO*, Hep_3, Hex_3, PEA_2, (P + PEA, or HexNAc)[b]
1851	1852	KDO*, Hep_3, Hex_5, PEA_2
2093	2094	KDO*, Hep_3, Hex_6, PEA, (P + PEA, or HexNAc)[b]

[a] KDO* refers to anhydro-KDO and P stands for phosphate. [b] (P + PEA) and HexNAc have the same nominal mass increment of 203 Da.

Oligosaccharides derived from the LOS of human mucosal pathogens generally consist of a limited number of common sugars, including hexose (Hex), *N*-acetylhexosamine (HexNAc), heptose (Hep), and 3-deoxy-D-*manno*-octulosonic acid (KDO), phosphate, phosphoethanolamine (PEA), and pyrophosphoethanolamine (PPEA) (Gibson et al., 1989; Phillips et al., 1990). *O*-Linked acetate groups are occasionally found on core HexNAc residues (John et al., 1991). A preliminary composition can often be assigned to an unknown OS by simple combination of these components.[3,4] In the present case,

[2] All masses are reported as the nominal mass of the ^{12}C-containing isotope unless otherwise noted.

[3] The residue masses for the ^{12}C-containing components of common LOS monosaccharides and other structural moieties are 162.05 (Hex), 203.08 (HexNAc), 192.06 (Hep), 220.06 (KDO), 291.10 (NeuAc), 42.01 (Ac), 123.01 (PEA), 79.97 (phosphate), and 202.98 Da (PPEA).

[4] A computer program was used (W. Hines, UCSF) that permits the determination of all possible compositions for an OS of specified molecular weight containing up to nine different structural moieties.

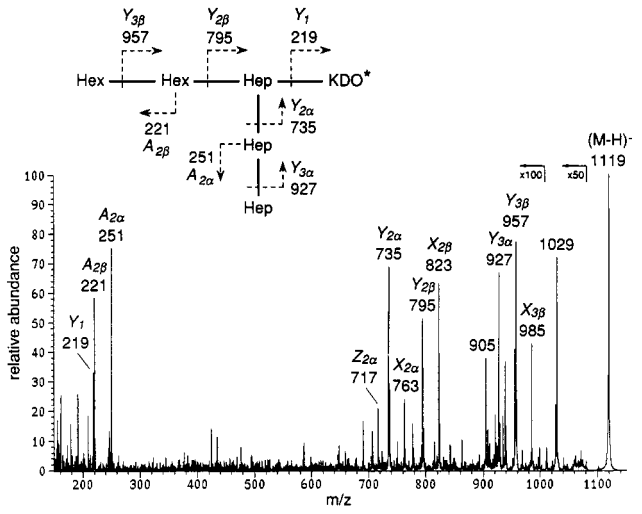

FIGURE 2: MS/MS spectrum of the major dephosphorylated hexasaccharide at $(M-H)^- = 1119$. Fragments are labeled according to the nomeclature proposed by Domon and Costello (1988). X, Y, and Z fragments arise from glycosidic bond or ring cleavages with charge retention at the reducing terminus; A, B, and C ions are nonreducing terminal fragments. The α and β subscripts distinguish the major and minor branches, respectively. Other sequence ions present but not labeled on the spectrum include m/z 955 ($X_{3\alpha}$), 939 ($Z_{3\beta}$), 909 ($Z_{3\alpha}$), 777 ($Z_{2\beta}$), and 247 (X_1). KDO* refers to anhydro-KDO. The large fragment ion at m/z 1029, $(M-H-90)^-$, is believed to result from ring cleavage of the reducing-terminal anhydro-KDO moiety.

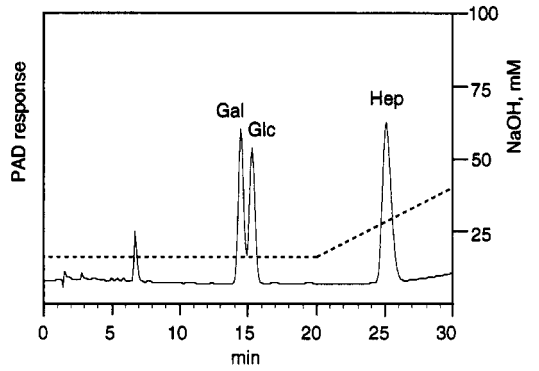

FIGURE 3: Monosaccharide components of the dephosphorylated NTHI 2019 hexasaccharide observed by high-performance anion exchange chromatography with pulsed amperometric detection. From comparison with monosaccharides obtained from hydrolyzed *S. typhimurium* Ra OS, a Gal:Glc:Hep ratio of 1.0:1.1:2.7 was measured for the NTHI 2019 OS. Conditions are as stated under Methods.

however, it was not possible to assign preliminary compositions to the NTHI oligosaccharides observed using only these residues. Additional experimental evidence (discussed below) led to the proposal that a KDO-like moiety, anhydro-KDO, exists on the reducing terminus of the NTHI 2019 oligosaccharides. With the incorporation of this residue, it was possible to generate proposed compositions for the majority of the OS molecular ions (Table II). All of the proposed structures possess a common core consisting of three heptoses and an anhydro-KDO moiety. Structural heterogeneity would appear to be confined to the phosphate substituents and branch saccharides.

Partial Structure of the Major Hexasaccharide Component. The major component of the NTHI 2019 oligosaccharides was a hexasaccharide (M_r 1366) with a proposed composition of two hexoses, three heptoses, two PEAs, and an anhydro-KDO (Table II). Dephosphorylation of this component with aqueous HF produced a new species of M_r 1120, indicating the removal of two PEA groups. To prepare a sufficient quantity of the dephosphorylated major component for structural studies, several fractions from the center and later-eluting side of the initial Bio-Gel P-4 column peak were pooled and HF-treated. The dephosphorylated material was then rechromatographed on a Bio-Gel P-4 column, and fractions were analyzed by LSIMS. Again, fractions were pooled across the center and later-eluting side of the Bio-Gel P-4 column peak in order to absolutely minimize contamination of the M_r 1120 component with higher molecular weight materials.

Negative ion tandem mass spectrometry was used to determine the sequence and partial structure of the major OS at M_r 1120 (m/z 1119). When selected for collision-induced dissociation, the parent $(M-H)^-$ ion at m/z 1119 produced the fragment ion spectrum shown in Figure 2. Fragment ions are identified following the nomenclature proposed by Domon and Costello (1988). Reducing terminal Y-type sequence ions resulting from glycosidic bond cleavages indicate that the molecular ion can lose either a nonreducing terminal Hex–Hex (m/z 957 and 795) or Hep–Hep (m/z 927 and 735) disaccharide. The Y_1 ion at m/z 219 arises from loss of the entire Hex_2Hep_3 moiety. This fragmentation pattern is consistent with a biantennary structure containing two nonreducing terminal disaccharide branches attached to a disubstituted heptose which is glycosidically linked to the reducing terminal anhydro-KDO moiety (Figure 2). These fragments, which account for the two hexoses and three heptoses in the proposed composition, support the assignment of an anhydro-KDO reducing terminal moiety with a residue mass of 202 Da. Additionally, the Hep–Hep branch establishes that the geometry of the Hep_3 core is different from the Hep_3 core found in *Salmonella* and *Escherichia coli* LPS. In these latter LPS (Galanos et al., 1977; Prehm et al., 1975), branching occurs from the penultimate heptose in a heptose trisaccharide structural moiety, rather than from the first heptose linked to the reducing terminal KDO. MS/MS analysis of the intact hexasaccharide (M_r 1366) indicated that the two PEA groups in the structure are present on the core. Fragments resulting from the loss of nonreducing terminal Hep(PEA) (m/z 1050) and a Hep(PEA)–Hep(PEA) branch (m/z 735) located one PEA group on each of the branch heptoses (data not shown).

To determine the precise monosaccharide composition of the major hexasaccharide, ≈15 nmol of the dephosphorylated sample were hydrolyzed and analyzed using high-performance anion exchange chromatography (Hardy et al., 1988) as shown in Figure 3. The NTHI 2019 sample was found to contain galactose and glucose in virtually equimolar quantities, as determined by comparison with a standard monosaccharide mixture containing $GalNH_2$, $GlcNH_2$, Gal, Glc, and KDO. L-*Glycero*-D-*manno*-heptose was identified in the sample by comparison (and co-injection) with the authentic monosaccharide liberated from the OS of *S. typhimurium* Ra. By comparing the areas of the three NTHI 2019 components with the corresponding monosaccharides present in the *S. typhimurium* sample, roughly 3 molar equiv of L-*glycero*-D-*manno*-heptose relative to 1 equiv of Gal and 1 equiv of Glc were contained in the NTHI 2019 OS (see the legend to Figure 3). Authentic KDO, which elutes at 43.2 min, was not detected in the hydrolyzed NTHI 2019 OS, although minor unidentified components which may be anhydro-KDOs eluted during the NaOAc gradient portion of the program (35–50 min). To further support the identification of L-*glycero*-D-*manno*-heptose, alditol acetates were also prepared. GC/MS analysis confirmed that only a single heptose-derived alditol acetate with retention time corresponding to the authentic hepta-*O*-acetyl-L-*glycero*-D-*manno*-heptitol was present in the NTHI 2019 OS sample.

Methylation analysis of the dephosphorylated major component was performed to determine monosaccharide linkage assignments. Again, the dephosphorylated OS from *S. typhimurium* Ra mutant was used as a standard. The partially methylated alditol acetate derivatives were analyzed by GC/MS using both EI and CI techniques. The NTHI hexasaccharide sample was found to consist of terminal galactose (1,5-di-*O*-acetyl-2,3,4,6-tetra-*O*-methylgalactitol), 1,4-linked glucose (1,4,5-tri-*O*-acetyl-2,3,6-tri-*O*-methylglucitol), terminal heptose (1,5-di-*O*-acetyl-2,3,4,6,7-penta-*O*-methylheptitol), 1,2-linked heptose (1,2,5-tri-*O*-acetyl-3,4,6,7-tetra-*O*-methylheptitol), and 1,3,4-linked heptose (1,3,4,5-tetra-*O*-acetyl-2,6,7-tri-*O*-methylheptitol). GC/MS peaks for the terminal galactose and 1,4-linked glucose derivatives were of nearly equal intensity, consistent with the 1:1 molar ratio determined from monosaccharide composition analysis. A terminal galactose to terminal heptose ratio of ≈1.0 to 0.8 was measured relative to the normalized values obtained for the partially methylated alditol acetates from the *S. typhimurium* Ra mutant. GC/MS peaks for the 1,2-linked and 1,3,4-linked heptoses were comparable in size to the terminal heptose peak, but standards required to accurately quantify those components were unavailable. In addition to the terminal galactose, a small amount (<0.1 molar equiv) of terminal glucose was also detected in the NTHI sample. While this may arise from traces of the minor pentasaccharide (M_r 958) present in the NTHI 2019 OS mixture, a small amount of contaminating terminal glucose was also present in the partially methylated alditol acetate mixture derived from the *S. typhimurium* Ra. Taken together with the MS/MS data, these results are consistent with the following partial structure:

Gal1→4Glc1→3,4Hep1→anhydro-KDO
↑
Hep1→2Hep1

Origin of the Reducing Terminal Anhydro-KDO Moiety. Whereas gonococcal LOS (Gibson et al., 1989), meningococcal LOS (Michon et al., 1990), and the LOS from *S. typhimurium* Ra mutant (John & Gibson, 1990) have been shown to yield "intact" oligosaccharides when subjected to mild acid hydrolysis, the NTHI 2019 LOS produced exclusively OS species which appeared to lack authentic KDO. Furthermore, these oligosaccharides were less stable than the corresponding gonococcal OS. Size exclusion chromatography of the sample in ammonium acetate, followed by evaporation of the solvent in vacuo, led to partial conversion of the oligosaccharides to species 28 Da lower in mass. This degradation reaction (apparent loss of CO from anhydro-KDO) was observed to go to completion when the sample was allowed to stand at 4 °C overnight in 1 M NH_4OH (pH 12), suggesting a base-catalyzed mechanism. Gonococcal OS, which are routinely chromatographed in 100 mM ammonium acetate (pH 7), do not undergo this degradation reaction.

Evidence that the NTHI 2019 OS did not contain authentic KDO was initially provided by composition and MS/MS analyses as discussed above. When the dephosphorylated major component from NTHI 2019 was derivatized with ethyl 4-hydrazinobenzoate (HBEE) and separated on reverse-phase HPLC as the corresponding hydrazone (John & Gibson, 1990), three major peaks and a few minor peaks were obtained (Figure 4A). Oddly, the major peaks all gave virtually the same LSIMS spectrum, with m/z 1281 as the most abundant molecular ion. From our previous experience, diastereomeric forms at the reducing terminus may be responsible for these multiple hydrazone-OS forms. Separation of the underivatized M_r 1120 OS using high-performance anion exchange chromatography produced a similar result of three closely eluting components (data not shown). When these peaks were collected and analyzed by negative-ion LSIMS, they all gave m/z 1119 as the major molecular ion. These results were consistent with microheterogeneity at the reducing terminal anhydro-KDO moiety.

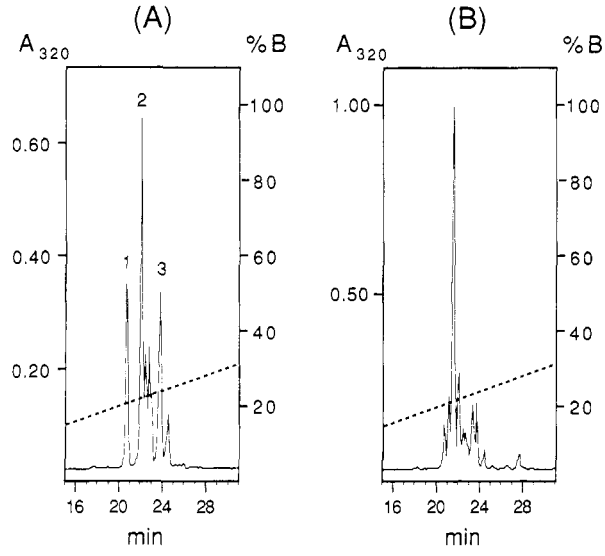

FIGURE 4: Reverse-phase HPLC chromatograms of NTHI 2019 OS derivatized with HBEE. (A) OS prepared by acid hydrolysis of LOS, followed by Bio-Gel P-4 purification and subsequent dephosphorylation. (B) OS prepared by dephosphorylation of LOS, followed by acid hydrolysis and Bio-Sil TSK purification. B is percent CH_3CN.

To rationalize the formation of diastereomeric anhydro-KDO structures in the NTHI 2019 hexasaccharide, a mechanism for their generation was sought. Elimination of a phosphate moiety from C-4 of KDO has been reported to occur during mild acid hydrolysis of intact LOS (Danan et al., 1982; Caroff et al., 1987). Loss of phosphate from the 4-position of KDO proceeds readily under these conditions because the C-4 substituent is β to the C-2 (anomeric) carbonyl carbon and can therefore undergo β-elimination. The reaction is believed to give rise to olefinic KDO derivatives, which can rearrange to form anhydro ring structures (Auzanneau et al., 1991). To ascertain whether elimination of a C-4 phosphate moiety from KDO might account for our results, OS was prepared from NTHI 2019 LOS using a modified method. Prior to acetic acid hydrolysis, the intact NTHI 2019 LOS was treated with aqueous HF to remove the phosphate esters. (Alternatively, the LOS was *O*-deacylated with hydrazine prior to HF treatment in order to increase its solubility in the aqueous solution.) Following removal of the aqueous HF, the dephosphorylated LOS was subjected to the standard mild acid hydrolysis conditions (1% acetic acid, 100 °C, 2 h), and the released oligosaccharides were fractionated on Bio-Sil TSK. LSIMS analysis of OS fractions revealed the presence of a new major component of M_r 1138 (m/z 1137). This OS was 18 Da larger than the previously obtained M_r 1120 OS generated from HF-treatment of the M_r 1366 OS and corresponded to a hexasaccharide composed of two Hex, three Hep, and one KDO. Clearly, the formation of this species using the modified method suggests that removal of an HF-labile moiety from the LOS prior to hydrolysis prevents formation of anhydro-KDO. In addition to the $(M-H)^-$ ion at m/z 1137, small amounts of the m/z 1119 species were also present in these fractions, which most likely arise from nonquantitative removal of the HF-labile moiety from KDO in the LOS.

A TSK-purified OS fraction containing the M_r 1138 species was derivatized with HBEE and chromatographed on re-

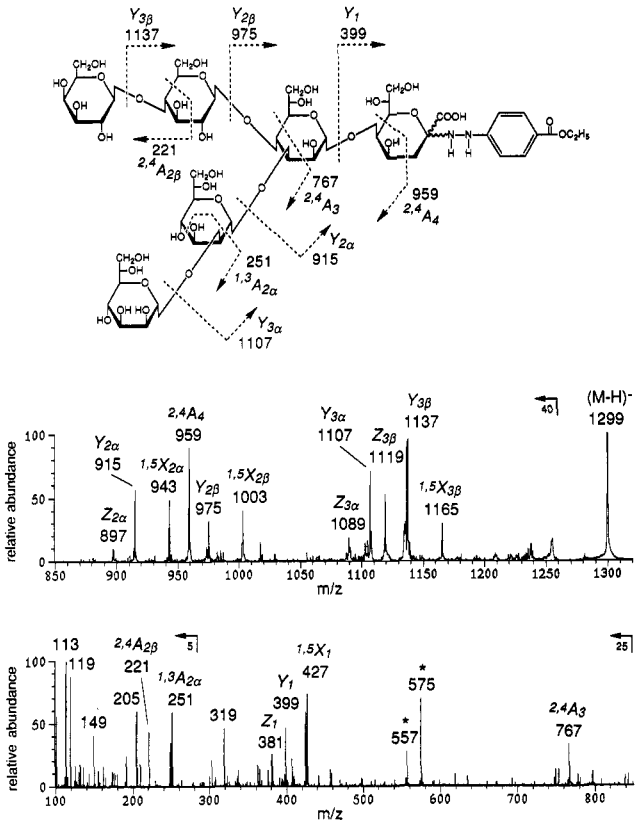

FIGURE 5: MS/MS spectrum of the major OS-HBEE component in Figure 4B at $(M-H)^-$ = 1299. Other sequence ions present but not labeled on the spectrum include m/z 1135 ($X_{3\alpha}$) and 957 ($Z_{2\beta}$). The ions labeled with asterisks appear to be Hep_3 fragments arising from cleavage of two glycosidic bonds. Linkage assignments and anomeric configurations indicated were derived from methylation analysis and NMR studies as discussed in the text.

verse-phase HPLC (Figure 4B). LSIMS analysis confirmed that the major component was an OS-HBEE derivative of M_r 1300, with the minor components corresponding to the previously obtained anhydro structures (M_r 1282). The MS/MS spectrum of the major component (Figure 5) supported the branching pattern deduced from MS/MS analysis of the underivatized, dephosphorylated anhydro structure (Figure 2). In this case, the derivatized sample exhibited more extensive fragmentation, including a complete series of nonreducing terminal A-type sequence ions. Furthermore, the MS/MS fragmentation pattern of the M_r 1300 OS-HBEE clearly defined a derivatized reducing terminal saccharide whose residue mass corresponds to authentic KDO.

Additional evidence for the presence of authentic KDO was provided by monosaccharide composition and methylation analyses of the M_r 1138 OS. Following hydrolysis, the sample was analyzed using anion exchange chromatography and found to contain authentic KDO. In order to determine the position of oligosaccharide linkage to KDO in the intact structure, the M_r 1138 OS sample was subjected to a modified methylation analysis reaction scheme designed to yield a partially methylated alditol acetate for reducing terminal KDO (York et al., 1985; John et al., 1991). When the M_r 1138 OS sample was treated in this fashion, a derivative resulting from 5-linked reducing terminal KDO (1,5-*O*-acetyl-2,4,6,7,8-*O*-methyl-3-deoxyoctitol) was obtained. The EI mass spectrum of this partially methylated alditol acetate was identical to the published spectrum of the 5-linked KDO derivative obtained from the OS of *N. gonorrhoeae* strain 1291_a (John et al., 1991). This result indicated that the 1,3,4-linked heptose residue in the NTHI 2019 OS is glycosidically linked to the C-5 of KDO and supports the hypothesis that an HF-labile moiety exists on the C-4 of KDO in the intact LOS.

Assignment of Anomeric Configurations and Branch Regiochemistry in the Hexasaccharide. The ^1H NMR spectrum of the major dephosphorylated hexasaccharide (M_r 1120; Hex_2, Hep_3, anhydro-KDO) reflected the sample microheterogeneity observed by chromatographic methods. Figure 6 shows the 500-MHz 1D ^1H NMR and DQF-COSY spectra. Although the structure should contain only five monosaccharide residues with anomeric protons, more than five resonances are visible in the anomeric region of the spectrum, consistent with several diastereomeric forms. Furthermore, the C-3 deoxy protons, which occur at high field (δ 1.9 and 2.2) and serve as markers for KDO (Caroff et al., 1987), were conspicuously absent, suggesting that the KDO moiety was altered such that the environment of the C-3 protons was significantly changed. With linkage data and MS/MS results available to define the partial structure of the NTHI 2019 hexasaccharide, it was possible to attribute complexities in the ^1H NMR spectrum to reducing terminal microheterogeneity (Auzanneau et al., 1991). Integration of the anomeric resonances suggested that the multiple signals could arise from a total of five protons existing in different subpopulations. On the basis of integrated areas (and coupling connectivities), the anomeric resonances were assigned to five spin systems (designated I, II, III, IV, and V) of three coexisting forms of the hexasaccharide structure as described below.

The anomeric resonances of spin systems III (δ 5.165, $J_{1,2}$ < 3 Hz) and V (δ 4.456, $J_{1,2}$ = 7.5 Hz) accounted for two anomeric protons which were not noticeably affected by the reducing terminal microheterogeneity. The most lowfield-shifted anomeric proton signal (II) consisted of three closely occurring broad peaks (δ 5.705, $J_{1,2}$ < 3 Hz; δ 5.682, $J_{1,2}$ < 3 Hz; δ 5.669, $J_{1,2}$ < 3 Hz) which together integrated for one proton. A set of three overlapping doublets (δ 4.556, $J_{1,2}$ = 7.5 Hz; δ 4.554, $J_{1,2}$ = 7.5 Hz; δ 4.546, $J_{1,2}$ = 7.5 Hz) integrated for another single anomeric proton (IV), and a group of three resolved broad peaks (δ 5.098, $J_{1,2}$ < 3 Hz; δ 5.080, $J_{1,2}$ < 3 Hz; δ 5.031, $J_{1,2}$ < 3 Hz) accounted for the final anomeric proton (I). The additional resonances present in the highfield end of the anomeric region (δ 4.611, J = 4.0 Hz; δ 4.476, J = 4.5 Hz; δ 4.404, $J \approx$ 2.5 Hz) were attributed to the anhydro-KDO moiety.[5]

On the basis of their chemical shifts and large coupling constants, the anomeric resonances of spin systems V (δ 4.456) and IV (δ 4.556, 4.554, and 4.546) were assigned to two β-linked saccharides. Given the composition of the OS, these resonances were readily attributed to the galactose and glucose residues, the only monosaccharides present with axial H-2 protons. The remaining lowfield-shifted broad peaks suggested α-linked *manno*-heptose residues. To distinguish these resonances, partial assignments of the galactose, glucose, and three *manno*-heptose spin systems present in the oligosaccharide were determined by application of DQF-COSY and 2D HOHAHA spectroscopy.

The anomeric proton at δ 4.456 was assigned to the galactose spin system (V) on the basis of the vicinal coupling constants measured for the H-1, H-2, H-3, and H-4 ring protons from cross-peaks in the DQF-COSY spectrum (Table III). The small $J_{3,4}$ coupling observed defines a sugar with the *galacto* configuration. The glucose spin system (IV) could

[5] When the OS was first dissolved in D_2O, these signals showed additional splitting and were coupled to resonances at δ 3.1–3.25. Prolonged sitting in D_2O fully exchanged the resonances at δ 3.1–3.25 and altered the splitting pattern of the coupled protons.

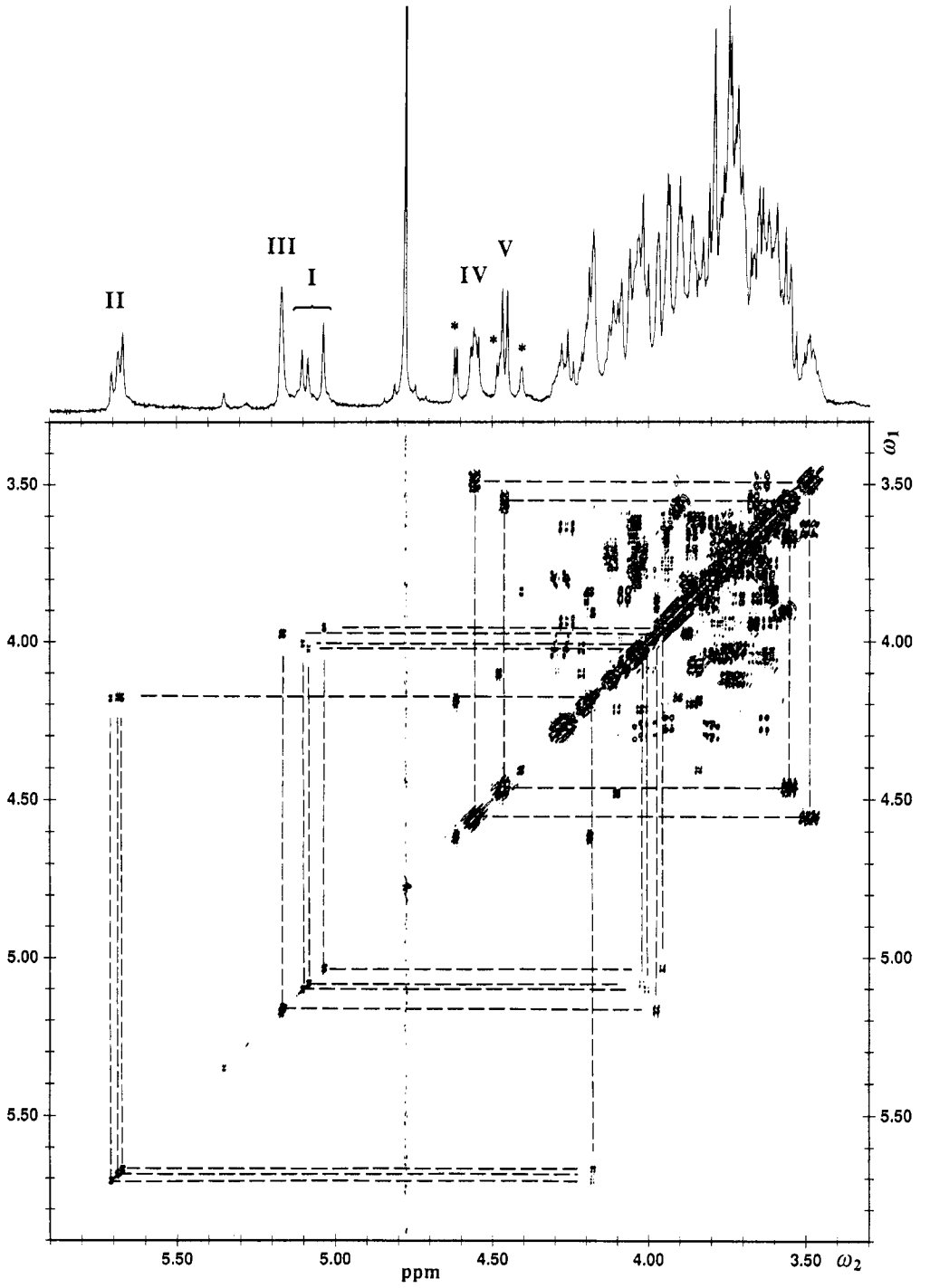

FIGURE 6: Section of the 500-MHz phase-sensitive DQF-COSY spectrum of 1.5 mg of the dephosphorylated hexasaccharide (M_r 1120) in 0.3 mL of D_2O at 25 °C. Negative contour levels are shaded. The 1D ^1H NMR spectrum is shown above the 2D data set, with anomeric protons labeled as shown in Table III and explained in the text. Cross-peaks correlating anomeric (H-1) and H-2 resonances are connected with dashed lines. Resonances in the anomeric region labeled with asterisks are believed to represent C-4 protons of 4,7- and/or 4,8-anhydro-KDO moieties (Auzanneau et al., 1991; Pozsgay et al., 1987). The peak at δ 4.78 is HOD.

only be mapped from H-1 (δ 4.556, 4.554, 4.546) to H-3 in the DQF-COSY spectrum. 2D HOHAHA spectroscopy was needed to reveal that the resonances for H-3, H-4, and H-5 are strongly coupled in this 1,4-linked β-glucose residue, as has been observed in related oligosaccharides (Michon et al., 1990; Inagaki et al., 1987). Figure 7A shows selected regions taken from below the diagonal in the 2D HOHAHA spectrum at the ω_1 frequencies of the anomeric resonances. Cross-peaks to the glucose anomeric proton show that magnetization transfer occurred throughout the entire spin system. The chemical shift of H-5 was measured from the H-5/H-6 cross-peak in the DQF-COSY spectrum, leaving the H-4 proton to be associated with the HOHAHA cross-peak at $\approx\delta$ 3.59.

All of the downfield-shifted anomeric resonances exhibited small $J_{1,2}$ couplings, consistent with α-linked saccharides. Protons H-1 (δ 5.165) to H-5 of III were assigned from the DQF-COSY and HOHAHA data (Figure 7A). The small $J_{2,3}$ coupling constant measured from the H-2/H-3 DQF-COSY cross-peak confirmed the *manno* configuration for this residue. The three signals assigned to the downfield-shifted anomeric proton of II (δ 5.705, 5.682, 5.669) all gave cross-peaks to about the same frequency in the DQF-COSY spectrum, consistent with their being assigned to the same mo-

Table III: Partial Proton NMR Assignment of the NTHI 2019 Hexasaccharide (D_2O, 25 °C)[a]

	V	IV		I		
	Galβ1→	4Glcβ1			4Hepα1→	*
			Hepα1→	2Hepα1	→3	
proton			III	II		
H-1	4.456	4.556	5.165	5.705	5.098	
		4.554		5.682	5.080	
		4.546		5.669	5.031	
H-2	3.55	3.49	3.97	4.18	4.01	
				4.18	4.02	
				4.18	3.95	
H-3	3.67	3.64	3.88	3.91	4.02	
				3.90	4.03	
				3.90	3.94	
H-4	3.94	≈3.59	3.80	3.59	4.28	
				3.57	4.29	
				3.56	4.26	
H-5	3.71[c]	≈3.62	4.03[b]	4.05[b]	3.80	
				4.05[b]	3.79	
				4.04[b]	3.63	
H-6		3.85			≈4.12[b,c]	
					≈4.13[b,c]	
					≈4.12[b,c]	
H-6′		4.08				
$J_{1,2}$	7.5[d]	7.5[d]	3	3	3	
$J_{2,3}$	10	9–10	4	sm[e]	3–4	
$J_{3,4}$	4		8	≈6	9–10	
$J_{4,5}$	sm[e]				10	

[a] Chemical shifts are reported in ppm. J values are apparent coupling constants (Hz) measured from DQF-COSY cross-peaks unless otherwise noted. The anhydro-KDO spin system (*) was not assigned, although downfield-shifted resonances appearing at δ 4.611, 4.476, and 4.404 were attributed to it (see Figure 6). [b] Tentative assignment from HOHAHA data. [c] Tentative assignment from NOESY data. [d] Coupling constants measured from the 1D spectrum. [e] Small coupling (unresolved in the DQF-COSY spectrum).

nosaccharide. Protons H-1, H-2, H-3, and H-4 of this spin system were mapped following COSY connectivities, with HOHAHA cross-peaks to the closely occurring anomeric signals providing a more reliable means of determining precise chemical shifts (Figure 7A). In this case, microheterogeneity caused overlap of DQF-COSY cross-peaks, permitting only approximate measurements of coupling constants for ring protons. The anomeric resonances assigned to I exhibited the greatest degree of chemical shift variation, suggesting that this residue was closest to the heterogeneous anhydro-KDO moiety. The H-1/H-2 cross-peaks in the DQF-COSY spectrum located the H-2 protons, but coupling connectivities could not be readily followed to H-3. Cross-peaks to the anomeric protons in the HOHAHA spectrum, however, suggested that the H-3 protons were strongly coupled to the H-2 protons in each case. With the H-3 protons revealed, connectivity to H-4 and H-5 could be followed in the DQF-COSY spectrum.

2D NOESY spectroscopy was used to determine the identities of the heptose residues and establish the location of branches on the trilinked heptose. Sections of the NOESY spectrum showing cross-peaks to anomeric protons are presented in Figure 7B. The anomeric resonances of *manno*-heptose residues I, II, and III all showed intraresidue NOE cross-peaks to their respective H-2 protons, consistent with the *manno* configuration. In addition to this coupling, H-1 of terminal heptose residue III showed interresidue NOEs to H-2 and H-1 of residue II. Interresidue NOEs between two anomeric protons are characteristic of 1,2-linkages in the α-configuration (Romanowska et al., 1988). H-1 of residue II showed an interresidue NOE to H-3 (and possibly H-2) of

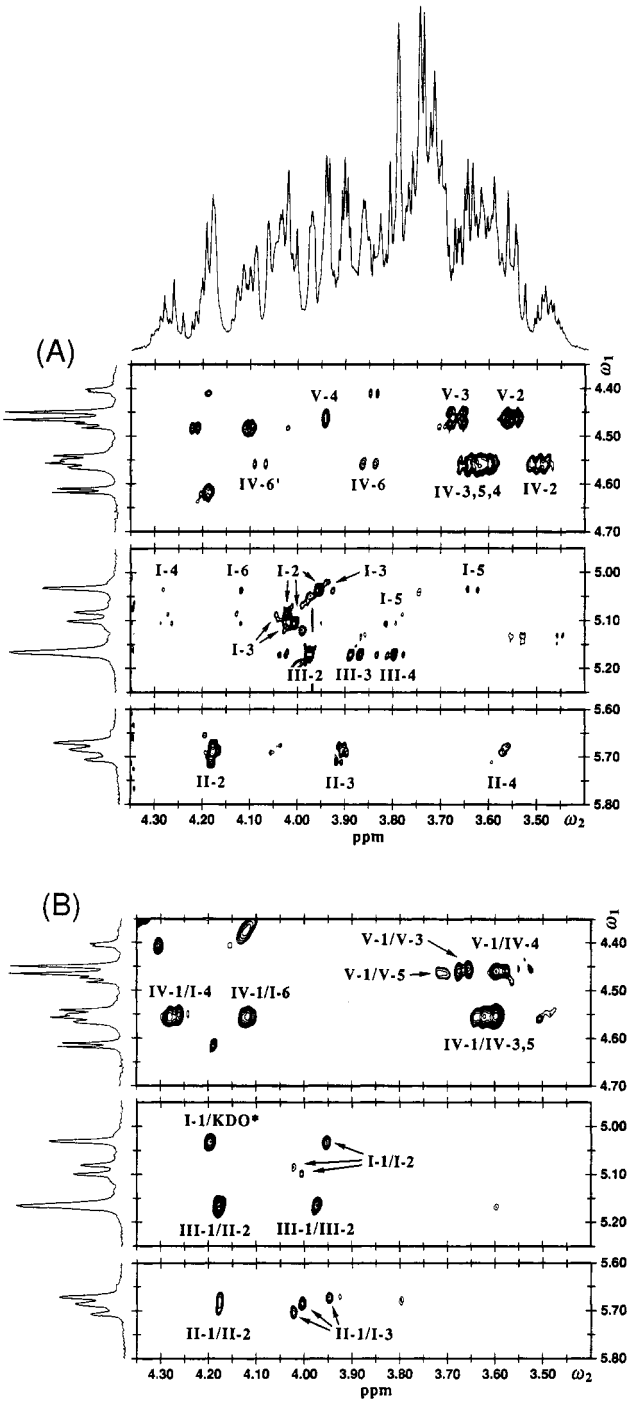

FIGURE 7: (A) Selected regions of the 2D HOHAHA spectrum of the dephosphorylated hexasaccharide in 0.3 mL of D_2O at 25 °C, acquired with a 90-ms mixing time. The middle and lower sections were plotted at lower contour levels than the upper section. Regions of the 1D spectrum are shown above and beside the 2D plots and cross-peaks to anomeric protons are labeled. Roman numerals represent sugar residues and numbers refer to proton assignments. (B) Corresponding regions of the 2D NOESY spectrum acquired with a 400-ms mixing time. All sections were plotted at the same contour levels. A NOE cross-peak between III-1 and II-1 is present in the full spectrum. Assignments of I-6 and V-5 are tentative.

residue I, establishing that II is linked to the 3-position of I. The anomeric proton of terminal β-galactose residue V showed an intraresidue NOE cross-peak to H-3 and interresidue coupling to the H-4 proton of IV. An additional NOE cross-peak to the anomeric proton of V was tentatively assigned to H-5 of V, a proton which could not be assigned from the DQF-COSY and HOHAHA data. The anomeric proton of

β-glucose residue IV showed intraresidue NOE cross-peaks to H-3 and H-5 and interresidue couplings to H-4 of residue I and a resonance tentatively assigned to H-6 of I. This supported placing the Galβ1→4Glcβ1→ branch on the 4-position of I. One of the anomeric resonances assigned to residue I (δ 5.031) showed a NOE cross-peak to a signal tentatively assigned to the anhydro-KDO spin system (Figure 7B). However, the specific assignment of this heptose linkage to C-5 of authentic KDO was made on the basis of methylation analysis data (discussed above). With respect to the 1,3,4-linked heptose I, this branching pattern is clearly related to that observed in oligosaccharides from meningococcal and gonococcal LOS.

Analysis of O-Deacylated NTHI 2019 LOS. In order to confirm the existence of phosphorylated KDO in the LOS, mass spectrometric experiments were performed on modified LOS species. Crude NTHI 2019 LOS was *O*-deacylated by treatment with hydrazine and subsequently dephosphorylated. Without further purification, the *O*-deacylated, dephosphorylated LOS was analyzed directly by negative-ion LSIMS (spectrum not shown). A major molecular ion was seen at m/z 1911, with minor components at m/z 1991, 2073, and 2235. The predicted molecular weight for a molecule consisting of the dephosphorylated M_r 1138 hexasaccharide and an *O*-deacylated, dephosphorylated lipid A moiety bearing two *N*-linked 3-hydroxytetradecanoic acid residues is M_r 1912. The ion at m/z 1991 corresponds to the m/z 1911 component bearing a residual phosphate group (+80 Da), and the higher mass ions (m/z 2073 and 2235) represent species bearing additional hexose residues (+162 Da/Hex). Independent LSIMS analysis of the free NTHI 2019 lipid A (obtained by mild acid hydrolysis of intact LOS) produced a major molecular ion at m/z 1823, consistent with a lipid A structure consisting of a glucosamine disaccharide bearing four 3-hydroxytetradecanoic acid residues, two tetradecanoic acids, and two phosphates (spectrum not shown). Glucosamine, tetradecanoic acid, and 3-hydroxytetradecanoic acid were detected in compositional analyses of the NTHI 2019 lipid A (W. Melaugh, unpublished results), suggesting that the molecular weight and composition of this lipid A are consistent with the *H. influenzae* lipid A structure reported by Helander et al. (1988). Taken together, these LSIMS results suggested that only a single KDO links the OS to the lipid A moiety in NTHI 2019 LOS. In the LSIMS spectrum of the *O*-deacylated, dephosphorylated LOS, there was no evidence of species containing additional KDOs.

Attempts to analyze the intact *O*-deacylated NTHI 2019 LOS (with phosphate groups still present) using negative-ion LSIMS were not successful. Since two PEA groups are present on the OS structure, electrospray MS (Smith et al., 1990) in the positive-ion mode was attempted as an alternative means of producing stable molecular ions. The resulting spectrum contained a mixture of protonated and sodiated doubly and triply charged ions (spectrum not shown), consistent with an *O*-deacylated LOS bearing two PEA groups and three phosphate moieties (measured average mass, 2399.9 ± 0.6). Having demonstrated the existence of two PEAs on the OS moiety and two phosphates on the lipid A structure, we conclude from this electrospray MS data that a third phosphate group exists on the KDO moiety linking the lipid A to the OS (Figure 8). Again, no evidence was seen for additional KDOs in the LOS structure.

Discussion

SDS–PAGE indicated that the NTHI 2019 LOS consisted of one major component and several minor species. Mass

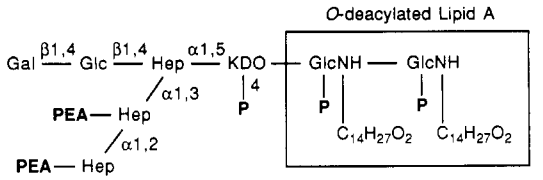

FIGURE 8: Proposed structure of the *O*-deacylated NTHI 2019 LOS derived from electrospray MS data and LSIMS analysis of the dephosphorylated species as discussed in the text. Phosphate (P) and phosphoethanolamine (PEA) substituents are shown in boldface type.

spectral studies of chemically modified LOS revealed that the major structure was a hexasaccharide ketosidically linked via a single bridging KDO to a lipid A moiety. In the native LOS, the bridging KDO is apparently phosphorylated on C-4. As a result of this substitution, acid hydrolysis of the intact LOS yields oligosaccharides with anhydro-KDO on the reducing terminus rather than intact KDO (Auzanneau et al., 1991). The demonstration that a species with intact KDO could be obtained from LOS that had been HF-treated prior to acetic acid hydrolysis confirmed that anhydro-KDO was generated as an artifact of the hydrolysis procedure. While the microheterogeneity associated with the anhydro-KDO moiety could have in principle been avoided by initial dephosphorylation of the LOS, efforts to produce a preparation completely free of the anhydro forms were unsuccessful.

The major dephosphorylated hexasaccharide was shown by tandem mass spectrometry, methylation analysis, and NMR studies to have the following structure:

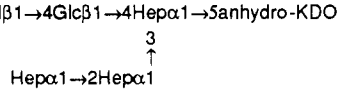

In the unmodified OS, both the terminal and dilinked heptose moieties are substituted with PEA. In addition to this species, we also observed higher molecular weight components in the NTHI 2019 OS mixture which most certainly contain different terminal epitopes. Methylation analysis of Bio-Gel P-4 fractions containing oligosaccharides larger than the major hexasaccharide component revealed additional sugars, including terminal glucose, 1,3-linked galactose, 1,2,3-linked heptose, terminal *N*-acetylglucosamine, and 1,4-linked *N*-acetylglucosamine. The presence of a second trilinked heptose moiety suggests that extension of the basal hexasaccharide structure may occur by elaboration of a new oligosaccharide branch from the 3-position of the penultimate heptose. Given the propensity of Hib LOS to undergo rapid phase variation (Kimura & Hansen, 1986; Kimura et al., 1987), it is possible that larger oligosaccharide structures may be more abundant in vivo. In a study of the LOS from Hib strain Eagan, Inzana et al. (1985) observed a major OS species of 1768 Da which was found to contain β-D-galactose and nonreducing terminal β-D-galactose linked to *N*-acetyl-D-galactosamine.

With the complete characterization of the dephosphorylated NTHI 2019 hexasaccharide and partial structural elucidation of the total LOS, we can begin to construct a structural model for *H. influenzae* LOS. Unlike the inner core structure of neisserial LOS, we have found a Hep_3-KDO core in the NTHI 2019 OS. The KDO is phosphorylated on C-4 and does not appear to be substituted with additional KDOs. This observation is interesting in connection with an earlier structural study conducted on the LPS of a deep-rough mutant strain of *H. influenzae* (strain I-69 Rd^-/b^+) whose oligosaccharide moiety was found to consist of only a single KDO, phosphorylated on either C-4 or C-5 (Helander et al., 1988). At the time, it was postulated that the phosphate substituents might

act as signals for (or blockers of) KDO-transferases and heptosyltransferases, which were reported to be lacking or inactive in the mutant strain (Helander et al., 1988). Our results are consistent with the hypothesis that phosphorylation on the 4-position of KDO prevents the addition of further KDOs to the core region of *H. influenzae* LOS. Alternatively, it is possible that species with additional KDOs would be too labile to give molecular ions under LSIMS or electrospray MS conditions, although we have previously observed intact LOS structures with two KDOs in *O*-deacylated, dephosphorylated gonococcal LOS (John et al., 1991; Phillips et al., 1990). Interestingly, phosphorylated KDO has also been observed in the LOS of *Bordetella pertussis*, the respiratory tract pathogen which causes whooping cough (Caroff et al., 1987, 1990).

Various Gram-negative pathogens share common epitopes (Campagnari et al., 1990; Virji et al., 1990). Recent studies have suggested that mucosal pathogens mimic host oligosaccharide structures in their LOS as a means of evading host defenses (Mandrell et al., 1988; Campagnari et al., 1990; John et al., 1991). The terminal lactose moiety (Galβ1→4Glcβ1→) present in the NTHI 2019 hexasaccharide is an epitope also present on lactosylceramide, a human glycosphingolipid and a precursor to human blood group antigens. Recently, a digalactoside moiety (Galα1→4Galβ1→) also found in mammalian glycolipid structures was detected on *H. influenzae* LOS using a monoclonal antibody specific for that epitope (Virji et al., 1990). Distinct from these terminal epitopes, a "KDO-related" epitope has been associated with NTHI 2019, as well as several recombinant *H. influenzae* strains (Campagnari et al., 1990; Spinola et al., 1990). While the genes coding for the expression of this epitope have been cloned (Spinola et al., 1990), the precise chemical structure of the epitope is not known. Further detailed studies of the LOS from additional strains *H. influenzae* will be needed to establish whether phosphorylated KDO may be a feature of this "KDO-related" epitope and identify other important epitopes involved in host/pathogen interactions.

Acknowledgments

We gratefully acknowledge the invaluable technical assistance of L. Reinders and thank members of the UCSF Mass Spectrometry (F. Walls and D. Maltby) and NMR Facilities (Drs. V. Basus, D. Banville, D. Kerwood, and S. Farr-Jones) for much help and guidance.

Registry No. Galβ1→4Glcβ1→(Hepα1→2Hepα1→3)4Hepα1→-5-KDO, 140148-99-8.

References

Auzanneau, F.-I., Charon, D., & Szabó, L. (1991) *J. Chem. Soc., Perkin Trans. 1*, 509.

Bax, A., & Davis, D. G. (1985) *J. Magn. Reson. 65*, 355.

Basus, V. J., Billeter, M., Love, R. A., Stroud, R. M., & Kuntz, I. D. (1988) *Biochemistry 27*, 2763.

Campagnari, A. A., Gupta, M. R., Dudas, K. C., Murphy, T. F., & Apicella, M. A. (1987) *Infect. Immun. 55*, 882.

Campagnari, A. A., Spinola, S. M., Lesse, A. J., Abu Kwaik, Y., Mandrell, R. E., & Apicella, M. A. (1990) *Microb. Pathog. 8*, 353.

Caroff, M., Lebbar, S., & Szabó, L. (1987) *Carbohydr. Res. 161*, c4.

Caroff, M., Chaby, R., Karibian, D., Perry, J., Deprun, C., & Szabó, L. (1990) *J. Bacteriol. 172*, 1121.

Danan, A., Mondange, M., Sarfati, S. R., & Szabó, P. (1982) *J. Chem. Soc., Perkin Trans. 1*, 1275.

Darveau, R. P., & Hancock, R. E. W. (1983) *J. Bacteriol. 155*, 831.

Di Fabio, J. L., Michon, F., Brisson, J.-R., & Jennings, H. J. (1990) *Can. J. Chem. 68*, 1029.

Domon, B., & Costello, C. E. (1988) *Glycoconjugate J. 5*, 397.

Falick, A. M., Wang, G. H., & Walls, F. C. (1986) *Anal. Chem. 58*, 1308.

Flesher, A. R., & Insel, R. A. (1978) *J. Infect. Dis. 138*, 719.

Galanos, C., Lüderitz, O., Rietschel, E. T., & Westphal, O. (1977) *Int. Rev. Biochem. 14*, 197.

Gibson, B. W., Webb, J. W., Yamasaki, R., Fisher, S. J., Burlingame, A. L., Mandrell, R. E., Schneider, H., & Griffiss, J. M. (1989) *Proc. Natl. Acad. Sci. U.S.A. 86*, 17.

Hardy, M. R., Townsend, R. R., & Lee, Y. C. (1988) *Anal. Biochem. 170*, 54.

Helander, I. M., Lindner, B., Brade, H., Altmann, K., Lindberg, A. A., Rietschel, E. T., & Zähringer, U. (1988) *Eur. J. Biochem. 177*, 483.

Inagaki, F., Kohda, D., Kodama, C., & Suzuki, A. (1987) *FEBS Lett. 212*, 91.

Inzana, T. J., Seifert, W. E., Jr., & Williams, R. P. (1985) *Infect. Immun. 48*, 324.

Jennings, H. J., Bhattacharjee, A. K., Kenne, L., Kenny, C. P., & Calver, G. (1980) *Can. J. Biochem. 58*, 128.

Jennings, H. J., Johnson, K. G., & Kenne, L. (1983) *Carbohydr. Res. 121*, 233.

John, C. M., & Gibson, B. W. (1990) *Anal. Biochem. 187*, 281.

John, C. M., Griffiss, J. M., Apicella, M. A., Mandrell, R. E., & Gibson, B. W. (1991) *J. Biol. Chem. 266*, 19303.

Kimura, A., & Hansen, E. J. (1986) *Infect. Immun. 51*, 69.

Kimura, A., Patrick, C. C., Miller, E. E., Cope, L. D., McCracken, G. H., Jr., & Hansen, E. J. (1987) *Infect. Immun. 55*, 1979.

Larson, G., Karlsson, H., Hansson, G. C., & Pimlott, W. (1987) *Carbohydr. Res. 161*, 281.

Levery, S. B., & Hakomori, S. (1987) *Methods Enzymol. 138*, 13.

Mäkelä, P. H. (1988) *Eur. J. Clin. Microbiol. Infect. Dis. 7*, 606.

Mandrell, R. E., Griffiss, J. M., & Macher, B. A. (1988) *J. Exp. Med. 168*, 107.

Marion, D., & Wüthrich, K. (1983) *Biochem. Biophys. Res. Commun. 113*, 967.

Michon, F., Beurret, M., Gamian, A., Brisson, J.-R., & Jennings, H. J. (1990) *J. Biol. Chem. 265*, 7243.

Moxon, E. R. (1990) in *Principles and Practice of Infectious Diseases* (Mandell, G. L., Douglas, R. G., Jr., & Bennett, J. E., Eds.) p 1722, Churchill Livingstone Inc., New York.

Moxon, E. R., & Vaughn, K. A. (1981) *J. Infect. Dis. 143*, 517.

Murphy, T. F., & Apicella, M. A. (1987) *Rev. Infect. Dis. 9*, 1.

Parr, T. R., Jr., & Bryan, L. E. (1984) *Can. J. Microbiol. 30*, 1184.

Patrick, C. C., Kimura, A., Jackson, M. A., Hermanstorfer, L., Hood, A., McCracken, G. H., Jr., & Hansen, E. J. (1987) *Infect. Immun. 55*, 2902.

Patrick, C. C., Pelzel, S. E., Miller, E. E., Haanes-Fritz, E., Radolf, J. D., Gulig, P. A., McCracken, G. H., Jr., & Hansen, E. J. (1989) *Infect. Immun. 57*, 1971.

Phillips, N. J., John, C. M., Reinders, L. G., Gibson, B. W., Apicella, M. A., & Griffiss, J. M. (1990) *Biomed. Environ. Mass Spectrom. 19*, 731.

Pozsgay, V., Jennings, H., & Kasper, D. L. (1987) *Eur. J. Biochem. 162*, 445.

Prehm, P., Strim, S., Jann, B., & Jann, K. (1975) *Eur. J. Biochem. 56*, 41.

Rance, M., Sorensen, O. W., Bodenhausen, G., Wagner, G., Ernst, R. R., & Wüthrich, K. (1983) *Biochem. Biophys. Res. Commun. 117*, 479.

Redfield, A. G., & Kuntz, S. D. (1975) *J. Magn. Reson. 19*, 250.

Romanowska, E., Gamian, A., Lugowski, C., Romanowska, A., Dabrowski, J., Hauck, M., Opferkuch, H. J., & von der Lieth, C.-W. (1988) *Biochemistry 27*, 4153.

Smith, R. D., Loo, J. A., Edmonds, C. G., Barinaga, C. J., & Udseth, H. R. (1990) *Anal. Chem. 62*, 882.

Spinola, S. M., Abu Kwaik, Y., Lesse, A. J., Campagnari, A. A., & Apicella, M. A. (1990) *Infect. Immun. 58*, 1558.

States, D. J., Harberkorn, R. A., & Ruben, D. J. (1982) *J. Magn. Reson. 48*, 286.

Stellner, K., Saito, H., & Hakomori, S. (1973) *Arch. Biochem. Biophys. 155*, 464.

Takayama, K., Qureshi, N., Hyver, K., Honovich, J., Cotter, R. J., Mascagni, P., & Schneider, H. (1986) *J. Biol. Chem. 261*, 10624.

Turk, D. C. (1982) in *Haemophilus influenzae, epidemiology, immunology, and prevention of disease* (Sell, S. H., & Wright, P. F., Eds.) p 1, Elsevier, Amsterdam.

van Alphen, L., Klein, M., Geelen-van den Broek, L., Riemens, T., Eijk, P., & Kamerling, J. P. (1990) *J. Infect. Dis. 162*, 659.

Virji, M., Weiser, J. N., Lindberg, A. A., & Moxon, E. R. (1990) *Microb. Pathog. 9*, 441.

Walls, F. C., Baldwin, M. A., Falick, A. M., Gibson, B. W., Kaur, S., Maltby, D. A., Gillece-Castro, B. L., Medzihradszky, K. F., Evans, S., & Burlingame, A. L. (1990) in *Biological Mass Spectrometry* (Burlingame, A. L., & McCloskey, J. A., Eds.) p 197, Elsevier, Amsterdam.

Yamasaki, R., Bacon, B. E., Nasholds, W., Schneider, H., & Griffiss, J. M. (1991) *Biochemistry 30*, 10566.

York, W. S., Darvill, A. G., McNeil, M., & Albersheim, P. (1985) *Carbohydr. Res. 138*, 109.

Zamze, S. E., & Moxon, E. R. (1987) *J. Gen. Microbiol. 133*, 1443.

Zamze, S. E., Ferguson, M. A. J., Moxon, E. R., Dwek, R. A., & Rademacher, T. W. (1987) *Biochem. J. 245*, 583.